

Supporting info for: Self-assembly of amphiphilic patchy particles with different cross-linking densities

Jing Zhang,^a Zhong-Yuan Lu,^{*a} and Zhao-Yan Sun^{*b}

Received Xth XXXXXXXXXXXX 20XX, Accepted Xth XXXXXXXXXXXX 20XX

First published on the web Xth XXXXXXXXXXXX 200X

DOI: 10.1039/b000000x

In this research, we present a simulation model for describing various cross-linking densities in two-patch particle matrix and/or in the two patches. The influence of cross-linking density on the self-assembly behavior of the patchy particles are examined in detail. In particular, two kinds of patchy particles are considered here, which are denoted by **PB-ML** (patchy particles with hydrophobic patches and hydrophilic matrix) and **PL-MB** (patchy particles with hydrophilic patches and hydrophobic matrix) in the following. In this *Supporting information*, we show all the parameters used in our simulations in section 1, quantify the relation between the simulation parameter and the solvent condition in section 2, show the self-assembly structures at different volume fractions in sections 3 and 4, and show equilibrium self-assembly structures of patchy particles in the cases of ultra-high and ultra-low cross-linking densities.

1 Simulation parameters

To describe the patchy particles, the bead-bead interactions are characterized by Lennard-Jones (LJ) type potential (Eqn. 1):

$$U_{LJ}(r) = 4\epsilon \left[\left(\frac{\sigma}{r} \right)^{12} - \left(\frac{\sigma}{r} \right)^6 \right], \quad (1)$$

and Weeks-Chandler-Anderson (WCA) potential (Eqn. 2):

$$U_{WCA}(r) = U_{LJ}(r) - U_{LJ}(r_c, WCA). \quad (2)$$

Actual simulation parameters used to describe the **PB-ML** and **PL-MB** particles are listed in Table 1 and Table 2, respectively.

2 Quantify the solvent quality

To quantify the solvent quality, we have checked the scaling between radius of gyration of the chain ($R_{g,c}$) and the chain length (N from 50 to 1000 with an interval of 50), $R_{g,c} \sim N^\nu$. The simulation parameters are listed in Table 3. In equilibrium, we have calculated $R_{g,c}$ and obtained the dependence of $R_{g,c}$ on N . We have found that $\nu = 0.314$ for using LJ potential between chain beads (i.e., bad solvent), and $\nu = 0.557$ for using WCA potential between chain beads (i.e., good solvent), as shown in Fig. 1.

^a Institute of Theoretical Chemistry, State Key Laboratory of Theoretical and Computational Chemistry, Jilin University, Changchun 130023, China. Fax: 0086 431 88498026; Tel: 0086 431 88498017; E-mail: luzhy@jlu.edu.cn

^b State Key Laboratory of Polymer Physics and Chemistry, Changchun Institute of Applied Chemistry, Chinese Academy of Sciences, Changchun 130022, China. Fax: 0086 431 85262969; Tel: 0086 431 85262896; E-mail: zysun@ciac.jl.cn

3 Equilibrium self-assembly structures of PB-ML particles

Fig. 2 and Fig. 3 show equilibrium self-assembly structures of **PB-ML** particles at volume fraction $\phi = 0.1$ and $\phi = 0.025$, respectively. Each patchy particle is represented by a sphere decorated with two patches. The spheres with the same color belong to the same cluster, and the sizes of the spheres are related to the swelling ratios. As can be seen from Fig. 2, the self-assembly structures are quite similar to the structures in the main text. For $\phi = 0.025$ as shown in Fig. 3, we can only obtain branched thread-like structures instead of three dimensional network even at high cross-linking densities. This is because the patchy particles have less chance to attractively interact with each other at low volume fraction.

4 Equilibrium self-assembly structures of PL-MB particles

As shown in main text, we can obtain better membrane morphologies when cross-linking only the matrix, so here we only show the self-assembly structures with this cross-linking scheme. Fig. 4 and Fig. 5 give equilibrium self-assembly structures of **PL-MB** particles at volume fraction $\phi = 0.15$ and $\phi = 0.05$ with detailed beads information, respectively. Patchy particles with same color belong to the same cluster. The self-assembly structures in Fig. 4 are quite similar to the structures in the main text. As shown in Fig. 5, some separated thin micelles instead of the bicontinuous membranes are obtained. Thus this volume fraction should be lower than the

gelation point for this system.

5 Equilibrium self-assembly structures of patchy particles in limiting situations

Fig. 6 shows equilibrium self-assembly structures of patchy particles in limiting situations. The self-assembly structures are quite similar to the structures in the main text when cross-linking density is very high. When cross-linking density is low, we obtain very disordered structures for **PB-ML** particles, while membrane structure with good morphology for **PL-MB** particles.

Table 1 Simulation parameters for **PB-ML** particles

Parameter	Value
Temperature	1.0
$\sigma_P = \sigma_M$	1.0
Potential type P-P	LJ
Potential type P-M	LJ
Potential type M-M	WCA
r_{LJ}	3.0σ
$r_{c,WCA}$	$\sqrt[6]{2}\sigma$
$\epsilon_{P-P} = \epsilon_{M-M}$	1.0
ϵ_{P-M}	0.2
$k_{harmonic}$	10.0
δt	5×10^{-3}
Total simulation steps	2×10^7
Thermostat	Brownian dynamics

P represents for patch bead
 M represents for matrix bead
 LJ represents for Lennard-Jones potential
 WCA represents for Weeks-Chandler-Anderson potential
 harmonic represents for harmonic bond potential

Table 2 Simulation parameters for **PL-MB** particles

Parameter	Value
Temperature	1.0
$\sigma_P = \sigma_M$	1.0
Potential type P-P	WCA
Potential type P-M	LJ
Potential type M-M	LJ
r_{LJ}	3.0σ
$r_{c,WCA}$	$\sqrt[6]{2}\sigma$
$\epsilon_{P-P} = \epsilon_{M-M}$	1.0
ϵ_{P-M}	0.2
$k_{harmonic}$	10.0
δt	5×10^{-3}
Total simulation steps	2×10^7
Thermostat	Brownian dynamics

Table 3 Simulation parameters for quantifying the solvent quality

Parameter	Value
Temperature	1.0
σ	1.0
ϵ	1.0
$k_{harmonic}$	10.0
δt	5×10^{-3}
Total simulation steps	1×10^6
Thermostat	Brownian dynamics

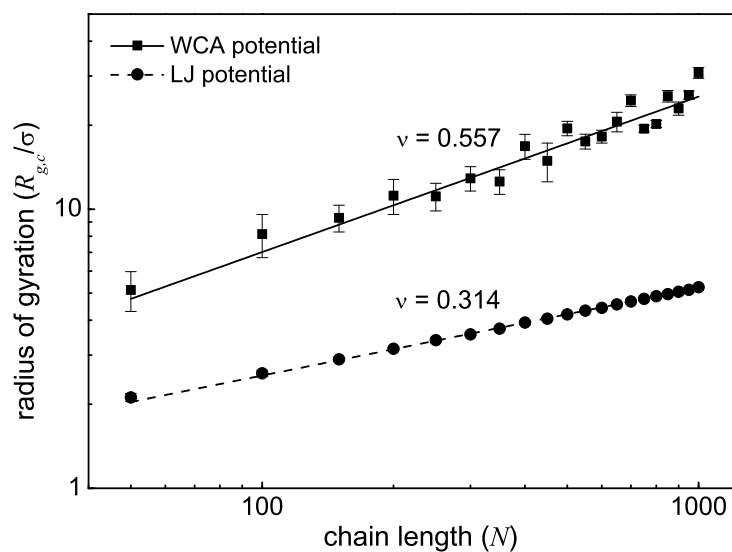


Fig. 1 Scaling law of radius of gyration of the chain ($R_{g,c}$) with the chain length (N from 50 to 1000 with an interval of 50), in which $R_{g,c} \sim N^\nu$. $\nu = 0.314$ for LJ potential (bad solvent), and $\nu = 0.557$ for WCA potential (good solvent).

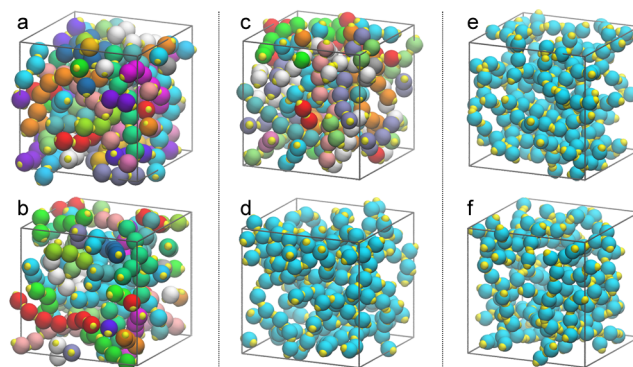


Fig. 2 Equilibrium self-assembly structures of **PB-ML** particles for the systems with different cross-linking densities $D_{c,m} =$ (a) 0.17, (b) 0.25, (c) 0.43, (d) 0.91, (e) 2.68, and (f) 4.33, at volume fraction $\phi = 0.1$. The spheres with the same color belong to the same cluster, and the sizes of the patchy particles are proportional to their swelling ratios.

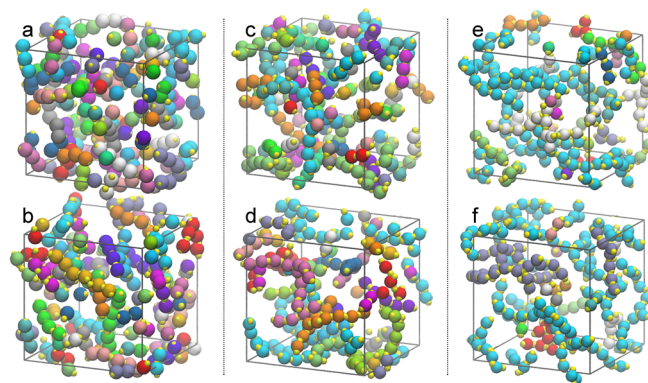


Fig. 3 Equilibrium self-assembly structures of **PB-ML** particles for the systems with different cross-linking densities $D_{c,m} =$ (a) 0.21, (b) 0.27, (c) 0.42, (d) 0.89, (e) 2.72, and (f) 4.31, at volume fraction $\phi = 0.025$. The spheres with the same color belong to the same cluster, and the sizes of the patchy particles are proportional to their swelling ratios.

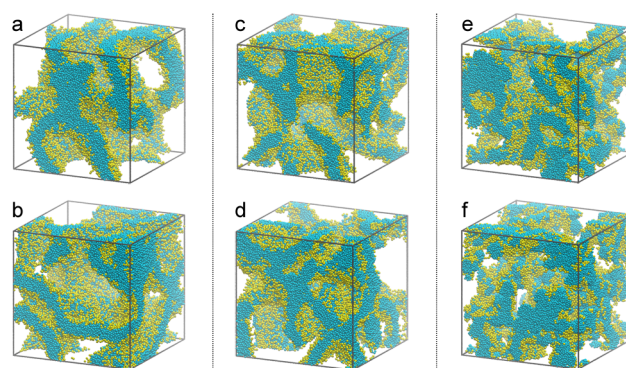


Fig. 4 Equilibrium self-assembly structures of **PL-MB** particles for the systems with different cross-linking densities $D_{c,m} =$ (a) 0.15, (b) 0.23, (c) 0.43, (d) 0.90, (e) 2.71, and (f) 4.33, at volume fraction $\phi = 0.15$ with detailed beads information.

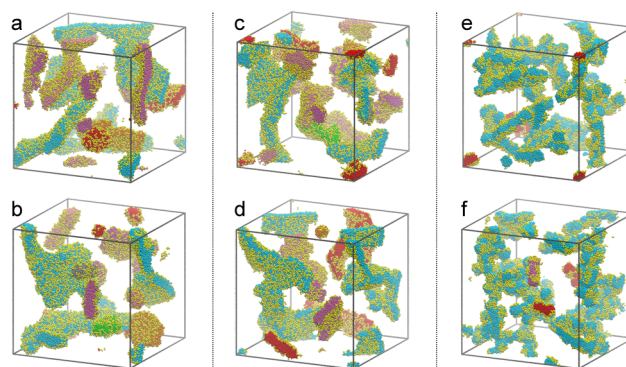


Fig. 5 Equilibrium self-assembly structures of **PL-MB** particles for the systems with different cross-linking densities $D_{c,m} =$ (a) 0.15, (b) 0.24, (c) 0.42, (d) 0.90, (e) 2.74, and (f) 4.28, at volume fraction $\phi = 0.05$ with detailed beads information.

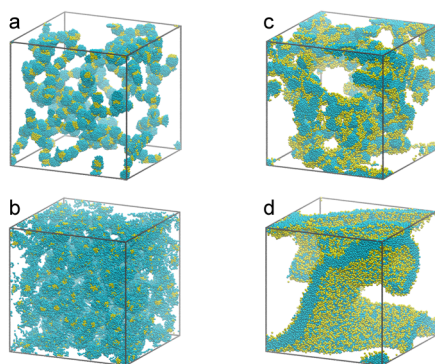


Fig. 6 Equilibrium self-assembly structures of **PB-ML** particles in limiting situations of $D_{c,m} =$ (a) 7.11, and (b) 0.04, at volume fraction $\phi = 0.05$. We also show the equilibrium self-assembly structures of **PL-MB** particles in limiting situations of $D_{c,m} =$ (c) 7.12, and (d) 0.06, at volume fraction $\phi = 0.1$.